Signatures of the hydrogen bonding in the infrared bands of water

J.-B. Brubach
LURE, UMR CNRS, bâtiment 209 D, Université Paris-Sud, 91405 Orsay cedex, France

A. Mermet
LPCML, UMR CNRS No. 5620 Université Lyon I-43, Boulevard du 11 Novembre 69622 Villeurbanne Cedex, France

A. Filabozzi
Dipartimento Fisica, Università Roma Tor Vergata and INFM, Via Ricerca Scientifica 1, 00133 Roma, Italy

A. Gerschel
LCP, UMR CNRS, bâtiment 490, Universite Paris-Sud, 91405 Orsay Cedex, France

P. Roy
LURE, UMR CNRS, batiment 209 D, Universite Paris-Sud, 91405 Orsay cedex, France and Synchrotron SOLEIL, I'Orme des merisiers Saint Aubin BP48, 91192 Gif sur Yvette Cedex, France

(Received 30 November 2004; accepted 24 February 2005; published online 9 May 2005)

Infrared spectroscopy measurements have been completed over a wide range of frequencies allowing to measure the evolution of both intramolecular and intermolecular vibrational modes in water as a function of temperature. Emphasis is made on the high frequency OH stretching band and the so-called connectivity band that lies in the far infrared region. The substructures of the two infrared bands are analyzed in terms of different levels of connectivity of the water molecules, along the statements of the percolation model. Both band profiles appear to be related to the different degrees of connectivity of water molecules. Comparison of the data with the predictions of the percolation model shows good agreement as for the temperature evolution of liquid water. This work provides additional support to the interpretation of water bands substructures as signatures of its very specific connectivity pattern. © *2005 American Institute of Physics*.
[DOI: 10.1063/1.1894929]

I. INTRODUCTION

Liquid water is a supermolecular assembly where individual constituent molecules are intercorrelated through both covalently bonded atoms, sustaining intramolecular vibrational modes, and noncovalently bonded atoms oscillating into intermolecular modes. The dynamical structure of liquid water is very peculiar: it consists of a robust three-dimensional network of highly versatile links (hydrogen bonds) that maintain the cohesion of the whole while constantly rearranging (breaking and reforming). Such pattern provides water with connective paths whose lifetimes are relatively short (~ picoseconds) and whose spatial extents spread over supermolecular distances. This picture implies that in an aqueous solution all processes occurring over a time scale lower than the average lifetime of the hydrogen bond networks "see" the water structure as an intricate network of connective channels. It is no doubt that these connective local structures play a significant role in the inner or interactive dynamics of nanoscopic biological objects.[1,2] Surprisingly, very little is known about this distinctive feature of water, in contrast with the relatively well-known chemistry of water molecules involved in biological environments.

The lack of experimental studies dedicated to the supramolecular connectivity of water arises from the low intensity of far infrared sources which makes difficult to directly probe the key element of this connectivity, the hydrogen bond. Because of its intermolecular nature and its supermolecular spatial extent, the vibrational characteristics of the hydrogen bond network lie in a rather low frequency range ($\omega \leqslant 300\ \mathrm{cm}^{-1}$). This spectral region can easily be reached through Raman[3–7] and infrared spectroscopies, although the lower wavenumber region ($\omega \leqslant 100\ \mathrm{cm}^{-1}$) becomes delicate to deal with for both experiments.[7–9]

An indirect way of probing the intermolecular network is to look at intramolecular modes of water molecules as their oscillator forces are sensitive to the level of interaction of the molecules with their surroundings. Indeed, it is quite generally observed that in a set of connected molecules, a change in the oscillator force of a particular bond induces correlated changes in the oscillator forces of the neighboring bonds (whether intramolecular or intermolecular). In the case of water, a most adequate tool to precisely detect such variations in bond oscillations is infrared spectroscopy due to the large transition dipole moment of water.

In previous studies, we had studied the evolution of water connectivity upon confinement through its midinfrared absorption spectrum.[10,11] The OH stretching band was analyzed in terms of several components, reflecting different populations of molecules involved in different levels of connectivity. Along this scheme of study, we have performed an infrared investigation of bulk water as a function of temperature (cooling), exploring both the intramolecular (OH stretching motion) and intermolecular (OH···O stretching

motion) spectral regions. We achieve a step further in the description of water connectivity by comparing our data with the predictions of the percolation model, whereby water molecules are distributed into five different classes differing from each other through their H-bond degree of coordination. We will show that this model allows a quantitative agreement with the percolation model for the O–H stretching bond and permits a qualitative description of the general evolution of the connectivity band.

The present paper is organized as follows. After a brief description of the experimental study, we present a qualitative overview of the infrared spectrum of water (from the far infrared end to the midinfrared region) together with its evolution towards crystallization. Then focus is made on the OH stretching band and on the so-called "connectivity band" ($\omega \leqslant 300$ cm^{-1}). The profile changes of both bands, observed upon cooling, are described in terms of connectivity variations making use of the percolation model.

II. EXPERIMENTAL SECTION

The infrared measurements were performed at the SIRLOIN beam line (Super-ACO, LURE). This beam line is equipped with a Bomem DA8 Fourier transform spectrometer and is able to operate either with internal IR sources or the synchrotron source.[12]

The midinfrared region ($500 \leqslant \omega \leqslant 9000$ cm^{-1}) was investigated thanks to a globar source, in combination with a KBr beam splitter and a Mercury Cadmium Telluride (MCT) wide range detector. The spectra were recorded with a resolution of 2 cm^{-1} with 200 scans per spectrum and no mathematical correction was further performed. Transmission measurements of both reference and sample were performed using a variable path cell (1 μm) using two diamond windows of 0.5 mm thickness. All spectra shown in the present paper display the infrared absorption coefficient defined as $A=-\log(I/I_0)$ where I_0 and I are, respectively, the transmitted intensity of the empty cell and that of the cell filled with water.

The far infrared region ($80 \leqslant \omega \leqslant 450$ cm^{-1}) was investigated thanks to infrared emission of synchrotron radiation provided by the ring Super-ACO, in combination with a composite Si beam splitter and a bolometer detector. The spectra were recorded with the same experimental parameters and setup as in the midinfrared region but with polyethylene windows.

In all cases, the temperature of the cell was controlled within ±0.1 °C.

III. EXPERIMENTAL RESULTS AND DATA ANALYSIS

A. Water IR spectrum upon cooling: Overview

The infrared spectrum of liquid water consists of four main bands, spreading between a few wavenumbers and ~3800 cm^{-1} (Fig. 1). The different spectral regions are experimentally reached with different setups (see preceding section).

The dominating feature of the IR water spectrum is the band located at 3400 cm^{-1} which corresponds to the stretching motion of the covalent OH bonds. Then, running the spectrum in decreasing frequency order, come the $\widehat{\text{HOH}}$ bending band ($\omega_{\text{bend}} \simeq 1650$ cm^{-1}), the libration band ($\omega_{\text{libr}} \simeq 675$ cm^{-1}), and the "connectivity" band ($\omega_{\text{conn}} \simeq 200$ cm^{-1}). While the former bands correspond to intramolecular modes, the latter ones more straightforwardly depend on the hydrogen bond: the libration mode, through small amplitude oscillations of the whole molecule, provides a mechanism of rupture and rearrangement of the hydrogen bonds at a subpicosecond rate. The connectivity band arises from the longitudinal motion of the hydrogen atom along the hydrogen bond axis (i.e., H-bond stretching) and therefore characterizes the level of H bonding between neighboring water molecules. The frequency position of the connectivity band matches well the end portion of the longitudinal phonon branch in liquid water.[13–15]

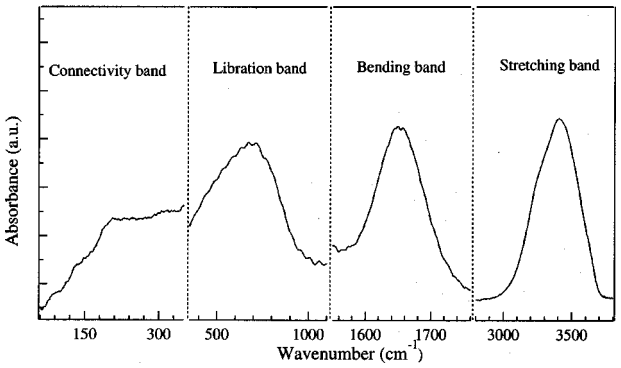

FIG. 1. Infrared absorption bands of liquid water at 298 K.

The evolution of the water spectrum upon cooling and subsequent crystallization is depicted in Fig. 2. As can be seen from this figure, the temperature behaviors of the different bands follow distinct trends.

(a) OH stretching band [Fig. 2(a)]: The shape of this band evolves significantly upon cooling. Upon crystallization (–8 °C in our experiment), the band is drastically modified with respect to its intensity, shape, and position ($\Delta\omega=120$ cm^{-1}). As will be further discussed in the following section, this band features several substructures that pertain to the different levels of hydrogen bonding of the water molecules.

(b) $\widehat{\text{HOH}}$ bending band [Fig. 2(b)]: Unlike the OH stretching band, this band decreases in intensity upon cooling and almost vanishes at the crystallization. Besides, as the temperature is lowered, the frequency of its maximum shifts towards higher frequency (+8%). The strong reduction of its intensity after crystallization most likely results from the loss of induced transition dipole moment through the bending motion. From this remark, one may suggest that, in the liquid phase, the bending band mostly reflects water molecules that do not lie in a symmetric tetrahedral environment. The single Gaussian shape of this band is a further indication that the bending mode is hardly sensitive to the different levels of connectivity of the water molecules.

(c) The libration band [Fig. 2(c), this band was measured with the combination of a KBr beam splitter and a

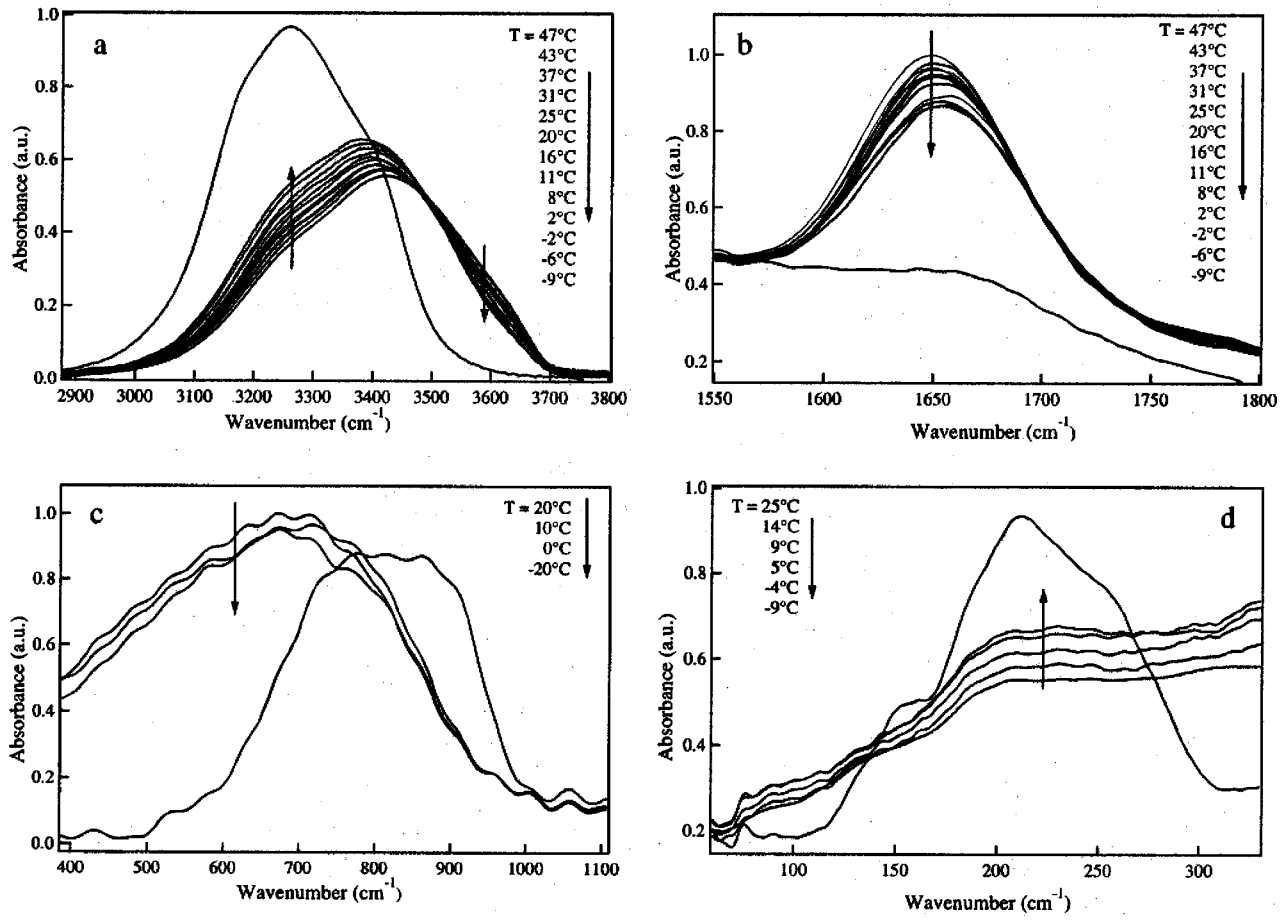

FIG. 2. Evolutions of the main bands of liquid water upon cooling and crystallization: (a) OH stretching band, (b) $\widehat{\mathrm{HOH}}$ bending band, (c) libration band, and (d) OH···O connectivity band. The intensities of the bands were arbitrarily rescaled. The fringes on (c) and (d) are due to multiple reflections in between the two sample windows.

bolometer detector]: Within the uncertainties of the data, the libration band remains approximately at the same position upon cooling while loosing intensity over its lower energy side. At the crystallization, the band profile is strongly modified and the position is shifted to higher frequencies passing from 675 cm^{-1} to 850 cm^{-1}. Unlike the bending motion, the librational motion remains active in the crystalline phase. The modest change with temperature in the liquid phase suggests that the frustrated rotation is little or not affected by the number of H bonds that the molecule establishes with its neighbors.

(d) The connectivity band OH···O [Fig. 2(d)]: This rather large structure emerges out of the low frequency tail of the libration band. Upon cooling, the band intensity increases quite significantly and undergoes a sharp modification at the crystallization. In both phases, the connectivity band exhibits several substructures, as will be discussed in more details in the next sections.

Among the four bands of water, two of them exhibit pronounced substructures that are seen to evolve upon cooling, they are the OH stretching band and the connectivity band. In the next sections, we show that in the liquid phase these substructures arise from the different levels of H bonding of water molecules.

B. The OH stretching band

The vibrational mode involving the stretching motion of the intramolecular OH bond is sensitive to the strength of the H bonding between water molecules. Within any sample of water, there exists a variety of molecules that are differently H bonded to each other, with H-bond coordination numbers ranging from 0 to 4. In a general way, the more H bonds a given molecule establishes with its neighbors, the weaker is its OH oscillator strength, and the more downshifted is the corresponding OH stretching frequency. On the basis of this argument, the substructures observed within the OH stretching band are ascribed to different populations of water molecules having different mean numbers of coordination. Analyzing the changes in profile of the band allows one to track the respective changes of the different populations, and therefore to get a more quantitative description of the water connective tissue. The evolving balance between these populations was investigated herein as a function of temperature.

Figure 3 displays the OH stretching band obtained for different temperatures ranging between 47 °C and −6 °C.

In the liquid phase, as temperature is decreased, the OH stretching band is seen to swell over its low frequency wing, leading to a shift of the band maximum towards lower energies (3419 cm^{-1} down to 3380 cm^{-1}) while the observed intensity increases by +16%. This small increase may be

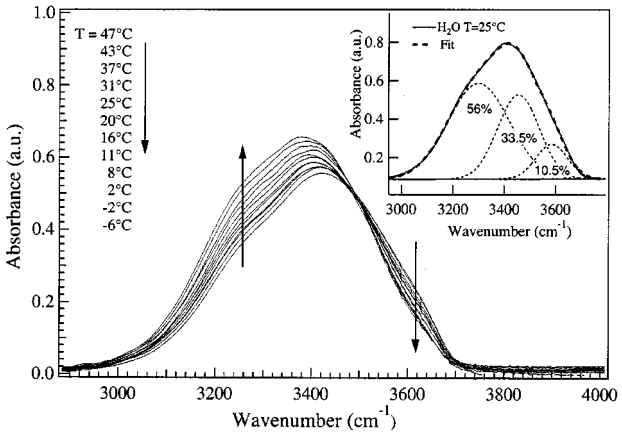

FIG. 3. OH stretching band of liquid water as a function of temperature. The inset shows the decomposition into three Gaussians at one temperature, with their respective relative areas.

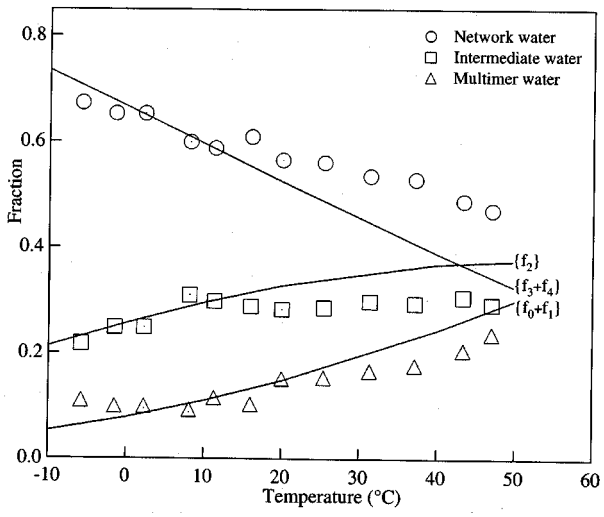

FIG. 4. Evolution of the three water populations (see text) as derived from a three Gaussian fit of the OH band. Solid lines show the temperature evolutions of the best matching sets of *j*-coordinated water molecules as derived from the percolation model.

linked to changes of density, transmission of window, and other experimental parameters. As often observed by both Raman[4,5,16] and infrared spectroscopies,[17] the O–H band spectra measured at various temperatures approximately cross each other in a "quasi-isobestic" point at 3480 cm^{-1}. In previous study,[5] this point was interpreted as the signature of two species of water molecules: H-bonded molecules and non-H-bonded molecules. We show below that this view can be reformulated in terms of balance between molecules that participate to the extended connective networks and those lying outside these networks.

As reported in previous studies,[3,10,11] the spectral profile of the OH stretching band can be very satisfactorily described by the superposition of several Gaussian components. As in the case of confined water in micelles, for example, Refs. 10, 18, and 19 a three-component analysis, although crude, provides extremely good fits to the data (see Fig. 3 inset), with a minimum number of parameters.[18–20] Although the three-Gaussian description is not unique, we show below that it provides a sound tool to quantitatively account for the changes of H bonding in water.

Following the above considerations on the OH bond oscillator strength as a function of the number of established H bonds, the three-Gaussian components were assigned to three dominating populations of water molecules. The lowest frequency Gaussian (ω=3295 cm^{-1}) is assigned to molecules having H-bond coordination number close to four, as this component sits close to the OH band observed in ice [see Fig. 1(a)]. The corresponding population is labeled "network water." Conversely, the highest frequency Gaussian (ω =3590 cm^{-1}) is ascribed to water molecules being poorly connected to their environment since the frequency position of this component lies close to that of multimer molecules (for instance, ω_{dimer}=3640 cm^{-1}).[21] This population is called "multimer water." In between the two extreme Gaussians lies a third component (ω=3460 cm^{-1}) which we associate with water molecules having an average degree of connection larger than that of dimers or trimers but lower than those participating to the percolating networks. This type of molecules is referred to as "intermediate water." Obviously, this picture describes a situation averaged over time and any one molecule is expected to belong to the three types of population over several picoseconds. The fact that the intermediate water Gaussian sits very close to the quasi-isobestic point frequency means, according to our view, that the quasi-isobestic point separates water molecules with respect to their involvement or noninvolvement in the long range connective structures, built up by almost fully bonded water molecules.

According to the three-Gaussian decomposition, free fits of the data were performed yielding different proportions of the three-Gaussian areas upon cooling. Notice that the position of each Gaussian remained constant within 1%. The Gaussian analysis requires only three components; three being the best compromise between a very satisfactory fit of the data at all the temperatures and a minimum number of fitting parameters. Other studies[22,23] did not evidence more than two components, possibly because they are based on difference spectra[23] or were obtained after Kramers–Kronig treatment of attenuated total reflection measurements.[22] Notice that these previous studies do not include a Gaussian analysis but are based on examination of zero crossing points. The relative proportions of the three Gaussians are plotted in Fig. 4 for 47 °C$\leqslant T \leqslant$–6 °C. The variations of the respective populations illustrate that even though "network water" is always the dominating population, its proportion steadily increases (48%–67%) as the temperature is lowered from 47 °C down to –6 °C. Simultaneously, the intermediate water contribution decreases from 30% to 21% while the multimer water proportion decreases from more than 24% to about 10%. These changes clearly evidence an increase of the organization of water towards a fully bonded network, as the crystallization point is approached.

Further insight into the evolution of this connectivity scheme can be gained by comparing the outcomes of the three-Gaussian analysis to the predictions of the percolation model developed by Stanley and Teixeira.[24] According to this model, the number of intact hydrogen bonds per mol-

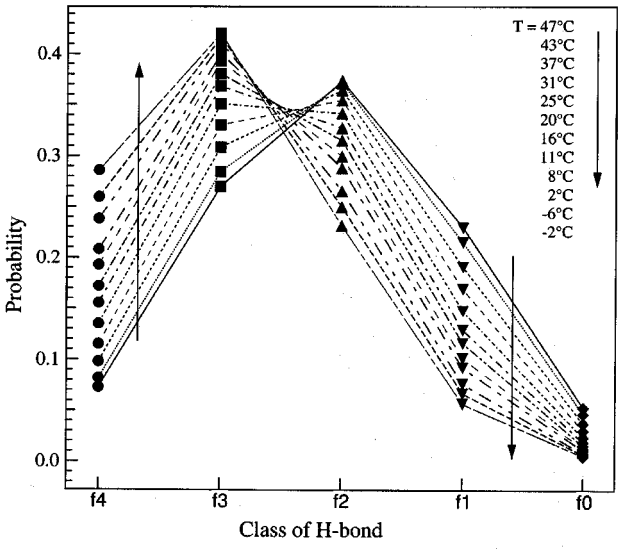

FIG. 5. Symbols: temperature evolutions of the fractions f_j corresponding to populations of j-coordinated water molecules.

ecule are given by the probability $p_B = n_{\mathrm{HB}}/z$ where n_{HB} is the number of established H bonds and z is the maximum number of hydrogen atoms bonded to one oxygen atom (covalent or intermolecular). We shall consider in the following that only a small minority of oxygen atoms are involved in more than four bonds with hydrogen atoms (two covalent and two H bonds), hence $z=4$. On the grounds of the percolation theory, the fraction f_j of water molecules having j H bonds is written as

$$f_j = \frac{z!}{j!\,(z-j)!} p_B^j (1-p_B)^{z-j}, \tag{1}$$

where j runs through 0 and 4. The temperature dependence of the coefficients f_j derives from the temperature dependence of p_B, as given by the empirical relation,[24]

$$p_B = 1.8 - 0.004T\ (\mathrm{K}) \tag{2}$$

provided that $-30\ ^\circ\mathrm{C} < T < 50\ ^\circ\mathrm{C}$.

Figure 5 illustrates the respective temperature variations of f_0, f_1, f_2, f_3, and f_4 over the temperature range of our study. One can see that from ~25 °C down, the dominating population is made of molecules establishing three hydrogen bonds while the mean degree of coordination is 2.4. Upon cooling, the fraction of four-bonded molecules f_4 strongly increases, while the three-bonded molecules f_3 tend to quickly pileup. The opposite evolutions are observed for the f_1 and f_2 fractions. Spectroscopically, the signature of the four-bonded molecules (f_4 class) is expected to lie at the lower energy end of the spectrum so that the abscissa in Fig. 5 can be conceived as a frequency axis.

Although our Gaussian analysis is based on only three components, it obviously shares some relationship to the five classes of molecules depicted in the percolation model ($f_0 \rightarrow f_4$). In order to compare the approaches, combinations of $\{f_i(+)f_j\}$ were searched in order to match the respective temperature variations of the three-Gaussian populations. These combinations are shown as lines in Fig. 4. It comes out that the temperature variations of the three sets $\{f_3+f_4\}$, $\{f_2\}$, and $\{f_0+f_1\}$ tend to, respectively, follow those of network water, intermediate water, and multimer water. As already suggested by our spectroscopic arguments, the low energy component of the OH band is confirmed to reflect water molecules connected to three or four other molecules, i.e., those molecules building up a supermolecular connective network. Water molecules establishing zero or one H bond are well described by the highest energy Gaussian and the intermediate water Gaussian corresponds to two-coordinated molecules. The relatively good quantitative agreement between the predictions of the percolation model and the three-Gaussian analysis definitely confirms that the substructures of the OH stretching band of water are indicative of the various degrees of connectivity of water molecules. Moreover, from Fig. 5, the crossing of the curves at $\{4,3\} \leqslant j \leqslant \{2,1,0\}$ supports once again that the quasi-isobestic point distinguishes between molecules belonging to an almost fully developed tetrahedral environment and molecules lying outside the connective networks.

IV. THE CONNECTIVITY BAND

The intermolecular motions involve noncovalent bonds that make up the cohesion of the supramolecular assemblies. Since the energies corresponding to these bonds are one or two orders of magnitude lower than those of covalent bonds, their spectral signatures range correspondingly at lower wavenumbers. The variety of the possible connections between water molecules, from the dimer to the tetrahedral coordinated network, provides the low energy vibrational spectrum of water with a certain degree of complexity. Only a few infrared studies have been attempted on the intermolecular bands of water[8,25,26] probably because of experimental difficulties arising from the very low intensities of infrared sources. In addition, the extreme low energy end of the spectrum features signatures of relaxation processes that compete with vibrational motions. Because of this the interpretation of the data obtained through different techniques (absorption, reflectivity, dielectric,…) do not always converge.

Figure 6(a) displays the variation of the connectivity band against temperature between 25 °C and –4 °C. It appears as a broad structure sumperimposed onto an increasing background. The overall appearance of the band shows substructures and gradually increases in intensity upon cooling. In comparison with the data of Zelsmann,[25] we note that (i) our data show more pronounced substructures and (ii) the substructure centered around 200 cm^{-1} becomes more pronounced upon cooling in agreement with Zelsmann's measurements[25] but unlike the evolution suggested by dielectric measurements.[26,27] The evolution we find in the cooling phase appears to be more in continuation with the changes induced by the crystallization, as is also the case for the three other bands (see Fig. 2). Notice that the dielectric studies[26,27] pointed out that part of the intensity of the band (at the lower energy end) is determined by relaxation processes (rotational and translational) of the water network in addition to the resonant stretching of the H bond described

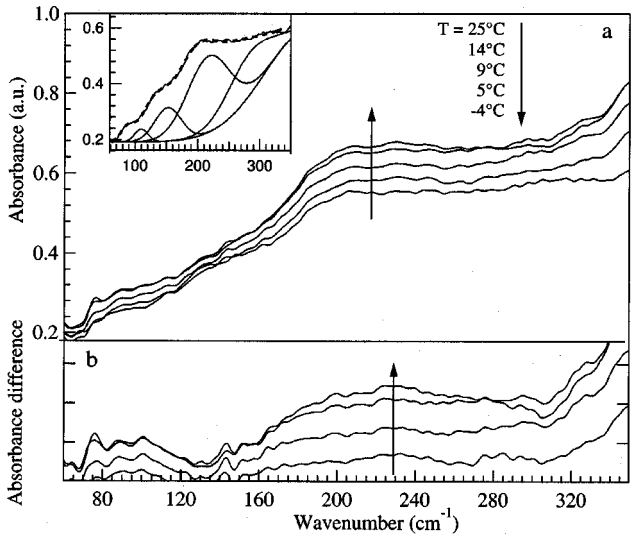

FIG. 6. (a) Evolution of the connectivity band of liquid water upon cooling. The inset shows a four Gaussian component analysis of the room temperature band, superimposed on the Gaussian wing of the libration band. (b) Difference absorbance curves, relative to the room temperature data.

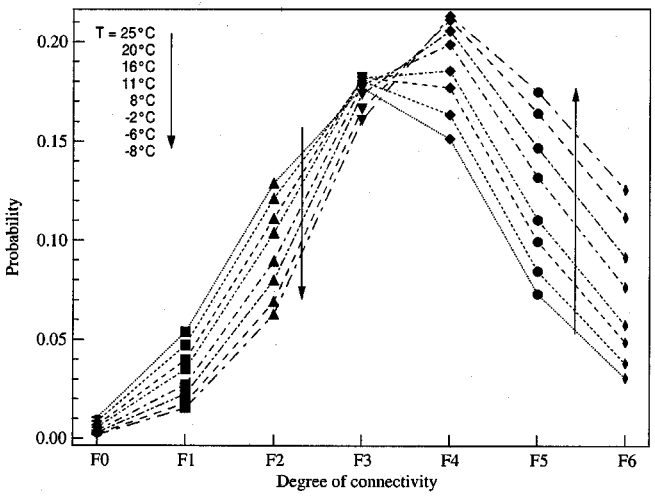

FIG. 7. Symbols: temperature evolutions of the fractions F_j corresponding to populations of j-coordinated sets of two water molecules.

above. The discrepancies with these dielectric studies and the infrared absorbance measurements may indicate a different sensitivity to the two types of absorbing processes amongst techniques.

In order to distinguish the evolution of the connectivity band from that of the background, difference spectra were determined, taking as reference the highest temperature measurement. This procedure allows to enhance the inelastic profile of the connectivity band with respect to the higher energy contribution. The results of the subtracting procedures are shown in Fig. 6(b). Three frequency regions appear to show distinct evolutions. The higher energy region ($\omega \geqslant 310\ \mathrm{cm}^{-1}$) steeply increases with decreasing temperature and is expected to arise from the libration changes. Clearly separated from this component is the middle region ($150 \leqslant \omega \leqslant 300\ \mathrm{cm}^{-1}$) unveiling a broadband whose intensity increases significantly upon cooling. At lower wavenumbers ($\omega \leqslant 140\ \mathrm{cm}^{-1}$), the variations appear to disclose a weak band, although the $\omega \leqslant 80\ \mathrm{cm}^{-1}$ data are to be considered with caution because of too small difference values and higher noise. Obviously, the broad middle feature is related to changes in the hydrogen bond network, reflecting a growing proportion of highly connected water molecules upon cooling.

The composite structure of the connectivity band is well fitted by a sum of four Gaussians superimposed on a rising monotonic background [Fig. 6(a) inset]. Free fits of the band for all temperatures yield constant positions at $\omega_1 = 88 \pm 1\ \mathrm{cm}^{-1}$, $\omega_2 = 130 \pm 1\ \mathrm{cm}^{-1}$, $\omega_3 = 195 \pm 1\ \mathrm{cm}^{-1}$, and $\omega_4 = 251 \pm 1\ \mathrm{cm}^{-1}$. Similarly to the OH stretching band analysis, these four components are expected to reflect different states of connectivity. However, in the case of the connectivity band, the highest energy component reflects water molecules having established a maximum of H bonds while it is the opposite in the case of the OH stretching band. This correspondence derives from cooperative effects according to which for a given set of molecules, the more H bonds are established, the stiffer the oscillator force. One can observe that the area of the connectivity band is directly related and proportional to the mean number of H bonds per molecule, as given by the percolation model, i.e., $A_{\mathrm{connect}}(T) \propto p_B(T) : p_B$ varies continuously from 0.61 at $T = 25\ ^\circ\mathrm{C}$ to 0.72 at $T \simeq -4\ ^\circ\mathrm{C}$, i.e., a relative increase of 18%. This value matches that of the relative intensity change of 19% as temperature is lowered in the same range, as evaluated after having removed the background contribution.

The evolution of the connectivity band, hence of the H bonding with temperature can also be addressed by the percolation model,[24] considering that the relevant basic unit is a set of *two* bonded molecules. For a couple of two bonded molecules, the number of links with other molecules lies between $Z = 0$ (this case corresponds to an isolated dimer) and $Z = 6$ (all bonds with neighboring molecules are established). It follows that the probability F_j for sets of two molecules having established j H bonds is given by

$$F_j = \frac{Z!}{j!\,(Z-j)!} p_B^j (1 - p_B)^{Z-j}, \tag{3}$$

where $Z = 6$ and j runs from 0 to 6.

The seven types of connectivity suggest that correspondingly the connectivity band can consist of up to seven states with various levels of established bonds ($F_0 \rightarrow F_6$). The temperature variations of the F_j states are presented in Fig. 7 for temperatures ranging between $T = 25\ ^\circ\mathrm{C}$ and $-8\ ^\circ\mathrm{C}$. The evolution of the curves reflect that as temperature is lowered the maximum of intensity moves towards states corresponding to more established bonds. Similarly to Fig. 5, and along the arguments developed above, the spectroscopic signature of the F_6 molecule set is expected to lie at the lower energy end of the spectrum.

The comparison of these curves with our data is not straightforward, mainly because of the contribution of the libration band which itself varies with temperature. However, both the percolation model and our experimental observations agree on two main trends: (i) the connectivity band is made up of three to four dominating substructures (F_3–F_5);

(ii) the higher energy substructures show the most rapid evolutions upon cooling. We notice that the experimental difference curves in the lower energy regions never reach negative values as would be expected from the calculated curves. The lack of quantitative agreement with the percolation model for the so-called connectivity band may indicate that the absorption in the 80–300 cm^{-1} region is determined not only by resonant processes (vibrations) but also by relaxation processes. Upon crystallization, the fading of intensity in the 80–120 cm^{-1} also suggests a relaxational origin.

V. CONCLUSION

The study of the infrared spectrum of water as a function of temperature shows that both intramolecular and intermolecular bands feature multicomponent structures that arise from the different degrees of connectivity of the molecules. The intramolecular OH stretching mode can be analyzed in terms of three Gaussians that allow to capture the essentials of the connectivity pattern of water. Such simple description is found to quantitatively fit with the five degrees of connectivity implied within the percolation model. Along these descriptions, crossing between the O–H band spectra measured at various temperatures and generally referred to as the quasi-isobestic point of the OH band is found to mark the boundary between molecules having a high degree of connectivity (more than two bonds per molecule) and those having a lower degree (less than two bonds) of connectivity. This view somewhat differs from the H-bonded/non-H-bonded equilibrium proposed earlier.[5]

Using the synchrotron infrared radiation, we were able to probe the low energy portion of the vibrational spectrum inherent to the stretching dynamics of the hydrogen bond. These data somewhat differ from previously published ones.[25] The so-called connectivity band also displays a multicomponent structure. The evolution of its integrated area upon cooling was found to be comparable to that of the mean number of hydrogen bond per molecule given by the percolation model. Although the change of the overall spectral shape of the band upon cooling (increase of the highest energy components) qualitatively agrees with inferences of the percolation model, a clear correlation to the different states of connectivity remains to be established. For such purpose, measurements covering a wider energy range, at both ends of the low energy spectrum (below 100 cm^{-1} and above 500 cm^{-1}), would be required. Experimental developments into this direction are currently under way. The present description of the various vibrational components may help characterize the level of connectivity in other systems where the water networks are expected to play an important role. Although this study used a limited number of subcomponents for this analysis, the general picture that emerges is a quasicontinuum of H-bonded interactions gradually changing with temperature and causing changes in the profile of O–H stretching and connectivity band.

[1] Y. Maréchal, J. Mol. Struct. **700**, 217 (2004).
[2] Y. Maréchal, J. Mol. Struct. **648**, 27 (2003).
[3] G. Walrafen, J. Chem. Phys. **47**, 114 (1967).
[4] G. Walrafen, M. Hokmabadi, and W. Yang, J. Chem. Phys. **85**, 6964 (1986).
[5] G. Walrafen, M. Fisher, M. Hokmabadi, and W. Yang, J. Chem. Phys. **85**, 6970 (1986).
[6] M. Nardone, M. A. Ricci, and P. Benassi, J. Mol. Struct. **270**, 287 (1992).
[7] J. Rousset, E. Duval, and A. Boukenter, J. Chem. Phys. **92**, 2150 (1990).
[8] J. B. Hasted, S. K. Husain, F. A. M. Frescura, and J. R. Birch, Chem. Phys. Lett. **118**, 622 (1985).
[9] T. Dodo, M. Sugawa, E. Nonaka, H. Honda, and S. Ikawa, J. Chem. Phys. **102**, 6208 (1995).
[10] J.-B. Brubach, A. Mermet, A. Filabozzi, A. Gerschel, D. Lairez, M.-P. Krafft, and P. Roy, J. Phys. Chem. B **105**, 430 (2001).
[11] C. Boissière, J.-B. Brubach, A. Mermet, G. de Marzi, C. Bourgaux, E. Prouzet, and P. Roy, J. Phys. Chem. B **106**, 1032 (2002).
[12] P. Roy, Y.-L. Mathis, S. Lupi, A. Nucara, B. Tremblay, and A. Gerschel, Synchrotron Radiat. News **8**, 415 (1995).
[13] F. Sette, G. Ruocco, M. Krisch, C. Masciovecchio, R. Verbeni, and U. Bergmann, Phys. Rev. Lett. **77**, 83 (1996).
[14] S. Saito and I. Ohmine, J. Chem. Phys. **102**, 3566 (1995).
[15] M. Sampoli, G. Ruocco, and F. Sette, Phys. Rev. Lett. **79**, 1678 (1997).
[16] G. D'Arrigo, G. Maisano, F. Mallamace, P. Migliardo, and F. Wanderlingh, J. Chem. Phys. **75**, 4264 (1981).
[17] H. Frank, *Water a Comprehensive Treatise* (Plenum, New York, 1972), Vol. 1.
[18] H. MacDonald, B. Bedwell, and E. Gulari, Langmuir **2**, 704 (1986).
[19] G. Onori and A. Santucci, J. Phys. Chem. **97**, 5430 (1993).
[20] P. Giguere, J. Chem. Phys. **87**, 4835 (1987).
[21] M. Thiel, E. Becker, and G. Pimentel, J. Chem. Phys. **27**, 486 (1957).
[22] T. Iwata, J. Koshoubu, C. Jin, and Y. Okubo, Appl. Spectrosc. **51**, 1269 (1997).
[23] F. Libnau, O. Kvalheim, A. Christy, and J. Toft, Appl. Spectrosc. **7**, 243 (1994).
[24] H. Stanley and J. Teixeira, J. Chem. Phys. **73**, 7 (1980).
[25] H. R. Zelsmann, J. Mol. Struct. **350**, 95 (1995).
[26] J. Vij, D. Simpson, and O. Panarina, J. Mol. Liq. **112**, 125 (2004).
[27] C. Rønne and S. Keiding, J. Mol. Liq. **101**, 199 (2002).